Delta expansion and Wilson fermions in the Gross-Neveu model: Compatibility with linear divergence and continuum limit from inverse-mass expansion

Hirofumi Yamada*
Education Center, Faculty of Information Science,
Chiba Institute of Technology,
Shibazono 2-1-1, Narashino, Chiba 275-0023, Japan
(Dated: December 5, 2015)

We apply δ-expansion to the Gross-Neveu model with Wilson fermions in the large N limit and investigate dynamical mass generation from inverse-mass expansion. The dimensionless mass M defined on the basis of the effective potential is utilized as the expansion parameter of the bare coupling constant β, which is partially renormalized by the subtraction of linear divergence. We show that the δ-expansion of the $1/M$ series of β is compatible with the mass renormalization. After confirmation of the continuum scaling of bare coupling without fermion doubling, we attempt to estimate dynamical mass in the continuum limit and, for range of Wilson parameter $r \in (0.8, 1.0)$, obtain results approaching to the exact value .

PACS numbers: 02.30.Mv, 03.75.Hh, 05.50.+q, 11.15.Me, 11.15.Pg, 11.15.Tk

I. INTRODUCTION

As well known, the system of real fermion fields on lattices with translational invariance, chiral symmetry and locality has been found to contain non-physical redundancy [1]. This no-go-theorem forbids any simple or straightforward fermion implementation into the lattice. The earliest proposal to circumvent this problem came from lattice inventor K. G. Wilson [2], who suggested breaking the chiral symmetry to the first order in the lattice spacing a. Among other proposals [3], Wilson's fermion system has an advantage in the strong coupling expansion, since his system enables an easy path to the expansion. The strong coupling expansion provides a simple, systematic and powerful computational scheme to clarify rich physics outside the scope of continuum perturbation theory. Pertaining to the approach where the continuum limit is accessed by the strong coupling series under the crucial help of δ-expansion [4–6], in this study we focus on the Wilson fermion system and investigate the recovery of asymptotic freedom and dynamical mass generation in a 2D lattice Gross-Neveu model in the large N limit [7].

In the formulation with auxiliary field σ_x, the action of the lattice Gross-Neveu model reads ($\mu = 1, 2$)

$$S = -\frac{a}{2}\sum_{x,\mu}\Big[\bar{\psi}_x(r-\gamma_\mu)\psi_{x+\mu} + \bar{\psi}_{x+\mu}(r+\gamma_\mu)\psi_x\Big] +2ar\sum_x \bar{\psi}_x\psi_x + a^2\sum_x \sigma_x\bar{\psi}_x\psi_x + \frac{Na^2}{2g^2}\sum_x(\sigma_x-\delta m)^2, \quad (1)$$

where ψ_x and g stand for the N flavor fermion on site x and the bare coupling constant, respectively. One choice for the explicit γ matrix is

$$\gamma_1 = \sigma_2, \quad \gamma_2 = \sigma_1, \quad \gamma_5 = \sigma_3 = i\gamma_1\gamma_2 \quad (2)$$

where

$$\sigma_1 = \begin{pmatrix} 0 & 1 \\ 1 & 0 \end{pmatrix}, \quad \sigma_2 = \begin{pmatrix} 0 & -i \\ i & 0 \end{pmatrix}, \quad \sigma_3 = \begin{pmatrix} 1 & 0 \\ 0 & -1 \end{pmatrix}, \quad (3)$$

and $\sigma_k^2 = 1$ $(k = 1, 2, 3)$. The parameter r is called the Wilson parameter and is kept at non-zero to avoid fermion species doubling. δm means the linearly divergent mass that is fixed by one-loop computation. The fermion propagator in the momentum space $(-\pi/a < p_\mu < \pi/a)$ reads

$$S_F(p) = \frac{1}{\sum_\mu i\gamma_\mu \frac{1}{a}\sin ap_\mu + \frac{r}{a}\sum_\mu(1-\cos ap_\mu)}, \quad (4)$$

where μ takes the values $1, 2$. The extra added term in S_F^{-1} due to Wilson behaves as $(1/2)ra\sum_\mu p_\mu^2$ near $p_\mu \sim 0$ and is negligible. At a corner of the Brillouin zone, $p = (\pi/a, \pi/a)$ for example, it behaves as $4r/a$ and grows to infinity as $a \to 0$. In addition of the four corners, the extra term behaves near the boundary of the Brillouin zone as $2r/a$ or $4r/a$ and behaves as the rest mass which goes on to infinity and decouples in the continuum limit.

Due to the explicit breaking of the γ_5 symmetry at $r \neq 0$, the radiative correction for the self energy diverges linearly and the counter term represented by $\delta m\bar{\psi}\psi$ must be accounted for. Explicit calculation specifies that

$$\delta m = -(2g^2/a)I \quad (5)$$

where I is given by

$$I(r) = \int_{-\pi}^{\pi}\frac{d^2p}{(2\pi)^2}\frac{r\sum_\mu(1-\cos p_\mu)}{\{r\sum_\mu(1-\cos p_\mu)\}^2 + \sum_\mu \sin^2 p_\mu}. \quad (6)$$

By introducing the mass counter term, the fermion stays massless to all orders of perturbative expansion.

The basic computational framework we take is the expansion in inverse powers of the mass suitably defined to be dimensionless with the combination of the lattice spacing a. Largeness of the mass M means largeness of the lattice spacing a, and therefore the $1/M$ expansion is equivalent with the

* yamada.hirofumi@it-chiba.ac.jp

strong coupling expansion. In the present work, first, we show that the mass renormalization is compatible with the large mass expansion even when the δ expansion is applied. This corrects the wrong statement in ref. [6] that the conventional truncation prescription of the δ-expansion fails to remove the linear divergence. We next confirm that the scaling of bare coupling (we do not perform full renormalization including the coupling constant, since thus far our approach depends solely on the bare quantities) is physical without fermion doubling. Then, we demonstrate that the mass computation can be approximately carried out from large mass expansion, which is valid in the large lattice spacings. With this detailed analysis of the δ-expansion to a solvable fermion model, we obtain further evidence of the effectiveness of δ-expansion combined with the large mass expansion.

II. ESTIMATION OF MASS FROM $1/M$ EXPANSION

A. Overview and strategy

The mass M used in this work is defined through the effective potential $V(\sigma)$. In the large N limit, the fermion integration is quadratic and results in

$$Va^2 = \frac{a^2(\sigma-\delta m)^2}{2g^2} - \int_{-\pi}^{\pi}\frac{d^2p}{(2\pi)^2}\log\Big[\sum_{\mu=1,2}\sin^2 p_\mu + (\sigma a + r\sum_{\mu=1,2}(1-\cos p_\mu))^2\Big]. \tag{7}$$

The mass m_D to be dynamically generated is given by $m_D = \sigma^*$ where σ^* denotes the solution of $dV/d\sigma = 0$. Then we define the dimensionless mass by

$$m_D a = M. \tag{8}$$

This reveals that $1/M$ expansion is an expansion effective at large lattice spacings. The continuum limit is apparently the limit $M \to 0$.

The necessary condition of the ground state $dV/d\sigma = 0$ gives the gap condition. It reads in terms of $M(= a\sigma^*)$ as

$$\begin{aligned} M &= a\delta m + 2g^2\int_{-\pi}^{\pi}\frac{d^2p}{(2\pi)^2}\frac{M + r\sum_\mu(1-\cos p_\mu)}{\{M + r\sum_\mu(1-\cos p_\mu)\}^2 + \sum_\mu \sin^2 p_\mu} \\ &= 2g^2\Big[-I(r) + \int_{-\pi}^{\pi}\frac{d^2p}{(2\pi)^2}\frac{M + r\sum_\mu(1-\cos p_\mu)}{\{M + r\sum_\mu(1-\cos p_\mu)\}^2 + \sum_\mu \sin^2 p_\mu}\Big] \end{aligned} \tag{9}$$

For a given positive value of g^2, there corresponds one value of $M(g^2, r)$. For example, as $g^2 \to 0$ in accord with the asymptotic freedom, $M \to 0$ as expected. There appears, however, the upper limit of M in the strong coupling limit $g^2 \to \infty$ due to the subtraction of linear divergence (In a large M region, the contribution of the counter term becomes dominant for any non-zero r). The limit $M(\infty, r)$ is smaller for larger r and larger for smaller r. For example, at $r = 1$, $M(\infty, 1) = 0.46732772346\cdots$. In the limit $r \to 0$, $M(\infty, r) \to \infty$. Thus, $1/M$ expansion covers both physical and unphysical regions.

Now, from (9), it follows that

$$\begin{aligned}\beta &:= \frac{1}{2g^2} \\ &= \int_{-\pi}^{\pi}\frac{d^2p}{(2\pi)^2}\frac{1 + r/M\sum_\mu(1-\cos p_\mu)}{\{M + r\sum_\mu(1-\cos p_\mu)\}^2 + \sum_\mu \sin^2 p_\mu} \\ &\quad -\frac{I(r)}{M}.\end{aligned} \tag{10}$$

For naive fermion at $r = 0$, $I(0) = 0$ and (10) gives $\beta = \int_{-\pi}^{\pi}\frac{d^2p}{(2\pi)^2}\frac{1}{M^2+\sum_\mu \sin^2 p_\mu}$. Thus, β becomes a function in the square of M rather than M itself. In bosonic cases such as the non-linear σ models and Ising models, the inverse coupling constant or the inverse temperature is described in the square of the mass. There exists a discrepancy in the suitable mass parameter between the present model at $r \neq 0$ and bosonic models.

Although the unphysical region is also covered, $1/M$ expansion for β, which we denote as $\beta_>$, is readily obtained as

$$\beta_> = -\frac{1}{M}I(r) + \Big\{\frac{1}{M^2} + \frac{-2r}{M^3} + \frac{-1+5r^2}{M^4} + O(M^{-5})\Big\}. \tag{11}$$

The above expansion becomes useless beyond the r-dependent convergence radius, and the small a behavior cannot be accessed. As discussed below, the δ-expansion changes the status in a drastic manner.

Suppose that $\beta_>$ is truncated at order n such that $\beta_{n>} = \sum_{k=1}^{n} b_k/M^k$. The result of the δ-expansion is summarized by

$$M^{-k} \to \binom{n}{k} t^k \tag{12}$$

with the binomial coefficient

$$\binom{n}{k} = \frac{n!}{k!(n-k)!}. \tag{13}$$

The δ-expansion induces an order-dependent transformation from $\sum_{k=1}^{n} b_k/M^k$ to the truncated series in t, $\sum_{k=1}^{n} b_n\binom{n}{k}t^k$. Let us use the notation $D[\beta_{n>}]$ or simply $\bar\beta_{n>}$ for the transformation of β. Then

$$\bar\beta_{n>}(t) = -I(r)\binom{n}{1}t + \Big\{\binom{n}{2}t^2 - 2r\binom{n}{3}t^3 + (-1+5r^2)\binom{n}{4}t^4 + \cdots + b_n\binom{n}{n}t^n\Big\}. \tag{14}$$

Here, b_n stands for the coefficient of $\beta_>$ at M^{-n}. Crucial advantage of $\bar\beta_{n>}$ is that it exhibits the scaling behavior within *its effective region at small* t. The rigorous specification of the effective region is not known but actually, the plots shown in Fig. 1 exhibit the expected logarithmic continuum scaling of $\bar{\beta}_{n>}$. As r decreases from $6/5$, the effective region

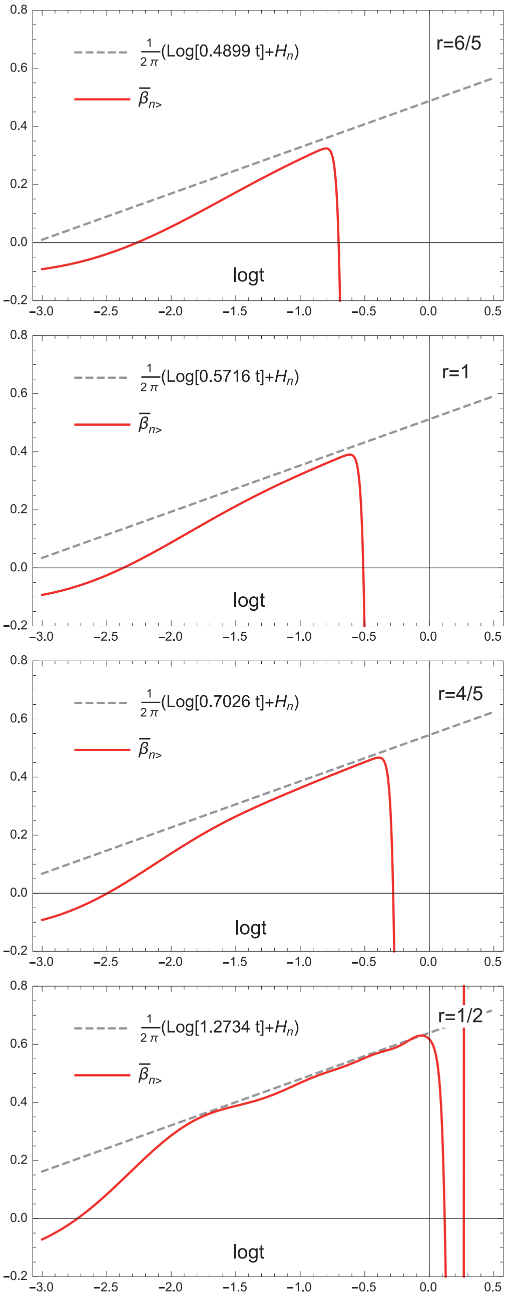

FIG. 1. Plots of $\bar{\beta}_{24>}$ and $\bar{\beta}_{24<} \sim 1/(2\pi)(\log(Ct) + H_{24})$ at $r = 6/5$ ($C = 0.4899$), $r = 1$ ($C = 0.5716$), $r = 4/5$ ($C = 0.7026$) and $1/2$ ($C = 1.2731$). Dashed line indicates continuum behavior at respective value of the Wilson parameter. The harmonic constant added to the logarithmic term comes from the δ-expansion.

of $\bar{\beta}_{n>}$ grows broader. However, as found from the 4th plot at $r = 1/2$, the behavior of $\bar{\beta}_{n>}$ becomes oscillatory. This oscillatory behavior becomes stronger for lower r. Note that the oscillatory behavior is a particular property in $\bar{\beta}_{n>}$, the δ expansion of the $1/M$ expansion, and not observable in the original exact function $\beta(M)$ given by (10).

The oscillation shows the fluctuation around the scaling behavior, which makes the estimation too complicated. Thus, we understand that there are preferred values of r. Within the range of these preferred values, the asymptotic freedom behavior of the bare coupling is observed and the matching of the behavior of $\bar{\beta}_{n>}$ with δ-expanded β in the scaling region would enable us to estimate critical quantities in the continuum limit. Although in ref. [6], we have wrongly stated that the cancellation of the first term in (14) (the counter term contribution from the linear divergence) with the expanded series, the rest set of (14), is incomplete, we correct this by stating here that the renormalization of the linear divergence is effective under the δ-expansion [8].

Most of the scaling behavior information near the continuum limit is governed by the ultraviolet structure of the model. For example, the logarithmic behavior with the coefficient $1/(2\pi)$ is found from the perturbative expansion. On the other hand, nonperturbative information such as the value of the dynamical mass cannot be reached merely from the results of perturbative series. In the Gross-Neveu model in the large N limit, the only quantity of nonperturbative nature included in the bare coupling is the dynamical mass to be generated. We propose that the information in $\bar{\beta}_{n>}$ effective at small t is enough to estimate the dynamical mass m_D. To make the estimation of m_D simpler and more accurate, we use the perturbative information of the ultraviolet divergence near the continuum limit in what follows.

We find from the perturbative renormalization group that the behavior of the bare coupling constant is

$$\beta(M) \sim \frac{1}{2\pi}\log(M/C), \tag{15}$$

with unknown constant C. Since the bare coupling should behave as $\beta(M) \sim \log(a\Lambda_L)/(2\pi)$ in the $M \to 0$ limit, we find

$$m_D = C\Lambda_L \tag{16}$$

where Λ_L stands for the mass scale on the square lattice. Thus the estimation of the constant C directly gives the dynamical mass.

The non-perturbative constant C depends on the Wilson parameter and consequently also on Λ_L, as m_D is universal. The non-universality of the scale Λ_L is natural since it depends on the microscopic construction of the lattice model. Analytically, C is obtained by the limit, $C = \lim_{M\to 0}\exp(\log M - 2\pi\beta(M))$. By the expansion of $\beta(M)$ given by (10) in the mass M, we then obtain

$$C = \exp[2\pi(c_1 - 2c_2)], \tag{17}$$

where

$$c_1 = \lim_{M\to 0}\Big[\int_{-\pi}^{\pi}\frac{d^2p}{(2\pi)^2}\frac{1}{(M+r\sum_\mu(1-\cos p_\mu))^2+\sum_\mu \sin^2 p_\mu}+\frac{\log M}{2\pi}\Big] \tag{18}$$

$$c_2 = \int_{-\pi}^{\pi}\frac{d^2p}{(2\pi)^2}\Big[\frac{r\sum_\mu(1-\cos p_\mu)}{(r\sum_\mu(1-\cos p_\mu))^2+\sum_\mu \sin^2 p_\mu}\Big]^2. \tag{19}$$

From numerical integration, we find that $C = 0.4899, 0.5716, 0.7026, 1.2731$ for $r = 6/5, 1, 4/5, 1/2$, respectively. These are the values used in the experimental plots in Fig. 1.

In the large N limit, the higher order corrections to the leading log form the lattice artifact which is a mixture of the powers of M and $\log M$. These terms can be computed if we use the closed result (10). However, using detailed information is not of real significance in our study, as our aim is to use only accessible information in the perturbation theory and the large M expansion. Hence, we here assume that

$$\beta_<(M) = \frac{1}{2\pi}\log(M/C) + R, \tag{20}$$

where R denotes the lattice artifact obeying $\lim_{M\to 0} R = 0$. The subscript "$<$" means the expansion at small M. For the matching of $\bar\beta_{n>}$ with the δ-expanded $\beta_<$, $D[\beta_<] = \bar\beta_{n<}$, we use the extension of the binomial coefficient by the Gamma functions,

$$M^\lambda \to \binom{n}{-\lambda} t^{-\lambda}, \tag{21}$$

where

$$\binom{n}{-\lambda} = \frac{\Gamma(n+1)}{\Gamma(-\lambda+1)\Gamma(n+\lambda+1)}. \tag{22}$$

Here λ denotes any real number. Taking λ infinitesimal in (21), we obtain $1 \to 1$ and $\log M \to -\log t - H_n$ where the harmonic number H_n is given by

$$H_n = \sum_{k=1}^{n}\frac{1}{k}. \tag{23}$$

The δ-expansion on $\beta_<(M)$ to the order n thus provides the transform

$$\bar\beta_{n<}(t) = -\frac{1}{2\pi}\{\log(Ct)+H_n\} + \bar R_n. \tag{24}$$

The matching of $\bar\beta_{n>}$ and $\bar\beta_{n<}$ enables us to estimate the constant C which directly gives the dynamical mass. The matching process is conveniently carried out through use of linear differential equation (LDE) to be approximately satisfied by $\bar\beta_{n<}$. The construction of the LDE needs, in a strict sense, the information of the lattice artifact $\bar R$. Though the explicit expansion from the gap equation (10) proves the existence of $M^\ell \log M$ as mentioned, we ignore it here and proceed in a robust manner to mimic the complicated structure with simple power like corrections,

$$\bar R = c_1 t^{-p_1} + c_2 t^{-p_1} + \cdots, \tag{25}$$

where $0 < p_1 < p_2 < \cdots$. Here we do not restrict the exponent p_k be an integer but rather let it possibly take a positive real number. In the estimation process of C based on LDE, the values of exponents will be optimized to non-integer value for the best matching.

Truncation of $\bar R$ to the first order gives $\bar\beta_{n<} = -\frac{1}{2\pi}\{\log(Ct)+H_n\} + c_1 t^{-p_1}$. The exponent of the logarithmic term is considered zero of double degeneracy. Thus, the ansatz with one-parameter obeys

$$\Big[0+\frac{d}{d\log t}\Big]^2\Big[p_1+\frac{d}{d\log t}\Big]\bar\beta_{n<} = 0. \tag{26}$$

In the matching region where the above LDE is valid, the function $\bar\beta_{n>}$ is also effective and approximately satisfies the same LDE as long as the order n is large enough. Hence, for large n, we deal with the same LDE for $\bar\beta_{n>}$,

$$\Big[0+\frac{d}{d\log t}\Big]^2\Big[p_1+\frac{d}{d\log t}\Big]\bar\beta_{n>} = 0, \tag{27}$$

and the integration over $\log t$ provides

$$\Big[1+p_1^{-1}\frac{d}{d\log t}\Big]\bar\beta_{n>} = -\frac{1}{2\pi}\{\log(Ct)+H_n\}, \tag{28}$$

and

$$\Big[1+p_1^{-1}\frac{d}{d\log t}\Big]\bar\beta_{n>} + \frac{1}{2\pi}(\log t + H_n) = -\frac{1}{2\pi}\log C. \tag{29}$$

To estimate C, we need to input values of p_1 and t around which point the LDE is considered to be satisfied. To obtain an optimal set of (p_1, t), we utilize an extension of the principle of minimum sensitivity (PMS) [9, 10]. We first demand that the estimation be done at the point t where the left-hand side of (29) is stationary with respect to t. We further demand that the reliable estimation point be in the scaling region, shown in this case as the plateau. Then, it is natural to utilize the second derivative of the left-hand side of (29) as zero or approximately zero at the best estimation point. These conditions are written as

$$\Big[1+p_1^{-1}\frac{d}{d\log t}\Big]\bar\beta^{(1)}_{n>} + \frac{1}{2\pi} = 0, \tag{30}$$

$$\Big[1+p_1^{-1}\frac{d}{d\log t}\Big]\bar\beta^{(2)}_{n>} \sim 0 \tag{31}$$

The symbol "$\sim$" in (31) means the exact or approximate equality (when a close point to zero exists). Note that the second condition (31) is nothing but (27). One can first solve (30) to give p_1 as the function of the stationary point t, $1/p_1 = \rho(t)$. Then, substituting the solution into the left-hand-side of (31), we can obtain one or several solutions.

TABLE I. Estimation result of $C = 0.5716061\cdots$ in 1- and 2-parameter ansatz at $r = 1$.

order n	20	30	40	50
1-parameter	0.5505666	0.5610658	0.5666871	0.5688271
2-parameter		0.5873315	0.5708970	0.5709232

Among them, the optimal one is identified by the value of t where all relevant functions $\bar{\beta}^{(\ell)}_{n>}$ for $\ell = 0, 1, 2, 3$ show expected scalings. For example, $\bar{\beta}_{n>}$ at $r = 1$ shows approximate scaling of about $t \sim 0.5$, and optimal solution t^* should be found around there. In these natural criteria, we can obtain only one solution at each order. Using the optimal solution t^*, we obtain $1/p_1^* = \rho(t^*)$ and from (29)

$$C = \exp\left[-2\pi(\bar{\beta}_{n>} + 1/p_1^*\bar{\beta}^{(1)}_{n>})|_{t^*} - (\log t^* + H_n)\right] \quad (32)$$

It is also possible to incorporate the next order correction t^{-p_2}. Then, the LDE with which we start reads as $[0 + \frac{d}{d\log t}]^2[p_2 + \frac{d}{d\log t}][p_1 + \frac{d}{d\log t}]\bar{\beta}_{n<} = 0$ and

$$\left[1 + p_2^{-1}\frac{d}{d\log t}\right]\left[1 + p_1^{-1}\frac{d}{d\log t}\right]\bar{\beta}_{n>} + \frac{1}{2\pi}(\log t + H_n) = -\frac{1}{2\pi}\log(C). \quad (33)$$

The extended PMS conditions read

$$\left[1 + p_2^{-1}\frac{d}{d\log t}\right]\left[1 + p_1^{-1}\frac{d}{d\log t}\right]\bar{\beta}^{(1)}_{n>} + \frac{1}{2\pi} = 0, \quad (34)$$

$$\left[1 + p_2^{-1}\frac{d}{d\log t}\right]\left[1 + p_1^{-1}\frac{d}{d\log t}\right]\bar{\beta}^{(2)}_{n>} = 0, \quad (35)$$

$$\left[1 + p_2^{-1}\frac{d}{d\log t}\right]\left[1 + p_1^{-1}\frac{d}{d\log t}\right]\bar{\beta}^{(3)}_{n>} \sim 0. \quad (36)$$

From the first two conditions, we obtain $p_1^{-1} + p_2^{-1} = \rho(t)$ and $(p_1p_2)^{-1} = \sigma(t)$ as functions of t and then, from the third condition, optimal $t = t^*$ can be obtained within the observable scaling region. The same as with one-parameter ansatz, we then obtain p_1^* and p_2^* and C from (33).

Next order correction t^{-p_3} is difficult to incorporate, since the necessary higher order derivatives $\bar{\beta}^{(\ell)}_{n>}$ ($\ell = 6, 7$) do not show scalings even at $n = 50$ (which is our limit), for practical reasons related to our computer facility.

B. Estimation at $r = 1$

We first confine ourselves to the popular choice $r = 1$. The results of estimation up to the 2-parameter ansatz are summarized in Table 1 and Fig. 2(a). Figure 2(b) plots the estimation results of p_1^{-1}.

We find that the sequence of the C-estimate shows a tendency to the exact value $C = 0.5716$. The speed of convergence is rather slow in 1-parameter ansatz. The estimate

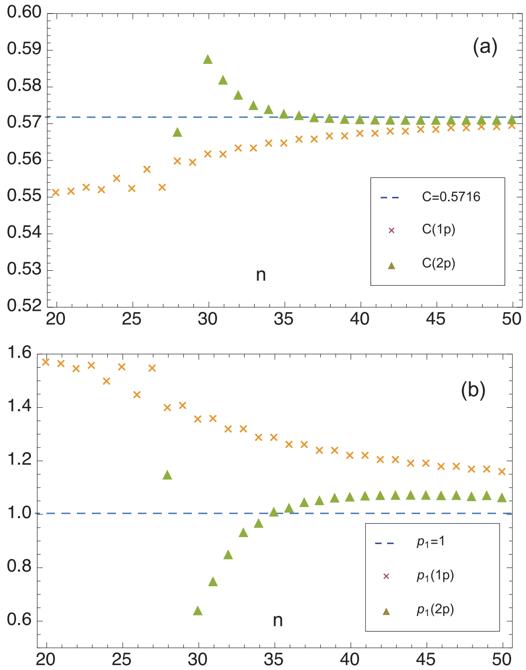

FIG. 2. Estimation results of (a) $C = 0.5716061\cdots$ and (b) $p_1 = 1$ in 1- and 2-parameter ansatz at $r = 1$. Plotted estimation is for $n = 20$ to 50.

in 2-parameter ansatz yields an accurate value but the onset of reliable estimation starts around the 35th order. The result of the p_1 estimate shown in Fig. 2(b) was obtained from the work of C-estimation as a byproduct. The limit of the sequence suggested is not yet clear. However, it is roughly approaching the value 1, which is actually the exponent of the leading order term in $\bar{R}$: In fact, from the exact result (10), R is given by $R = M(const + const\log M) + O(M^2)$. Then, $\bar{R} = const \times (1/t) + O(t^{-2})$, giving $p_1 = 1$.

We explored the possibility of the direct estimation of p_1 through $\bar{\beta}^{(3)}/\bar{\beta}^{(2)}$ showing scaling $\sim -p_1$. However, we failed because the ratio function exhibited large oscillation.

C. Estimation at $r \neq 1$

Now, we discuss our estimation work for $r \neq 1$. One might assume that the case $r = 1/2$ would provide better values, since the function $\bar{\beta}_{n>}$ is closer to $\bar{\beta}_{n<}$, as seen in the final plot in Fig 1. However, $\bar{\beta}_{n>}$ slightly oscillates at $r = 1/2$ and the derivatives would show oscillations with larger amplitudes. Actually, by explicit plots of $\bar{\beta}^{(\ell)}_{n>}$ ($\ell = 1, 2$), we find that the LDE approach does not work well due to the disturbing oscillation. Since incorporation of the derivatives is crucial for accurate estimation, this is a serious problem. From the plots of $\bar{\beta}_{n>}$ and the derivatives, we arrive at the following observation.

When r is larger than 1, the oscillation is absent but the effective range of $\bar{\beta}_{n>}$ is narrow, giving a less accurate estimate

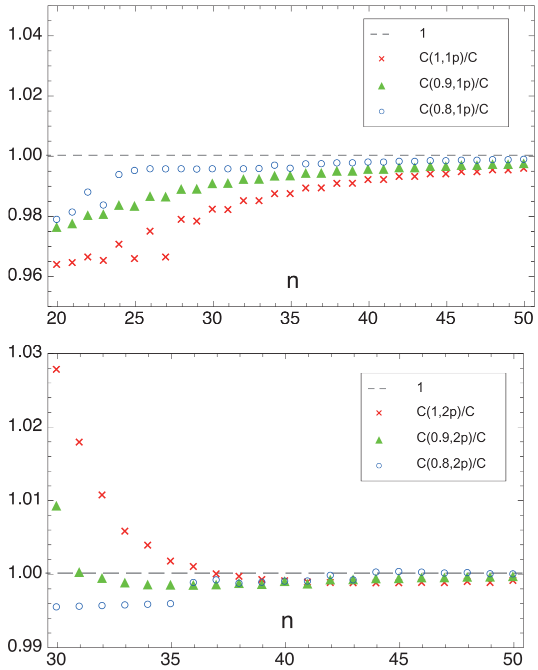

FIG. 3. Estimation results of C for $r = 1, 0.9, 0.8$ at 1- and 2-parameter ansatze (respectively plotted in the upper and lower parts). Here $C = 0.5716\cdots$, $C = 0.62797\cdots$ and $C = 0.7026\cdots$ for $r = 1, 0.9, 0.8$ respectively. The plots show the ratio of the estimate to the exact values.

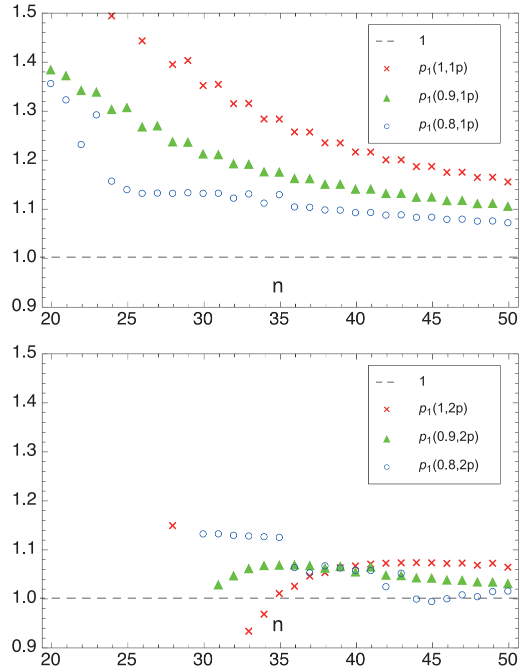

FIG. 4. Estimation results of $p_1 = 1$ for $r = 1, 0.9, 0.8$ at 1- and 2-parameter ansatze (respectively plotted in the upper and lower parts). Here, $p_1(r, kp)$ denotes the estimate at Wilson parameter r with k-parameter ansatz.

of C. When r is less than and close to 1, we observe a weak oscillatory property in $\bar{\beta}_{n>}$ and the derivatives at low orders. Although this makes the estimation slightly complicated, confirmation of the scaling region is possible. Around $r \sim 0.8$ or a slightly larger region, the scaling behavior in $\bar{\beta}^{(\ell)}$ is roughly visible in low order derivatives and the estimation protocol by extended PMS is permitted. The value $r = 0.8$ is the best among the three sample values. We confirmed that r smaller than 0.8 worsens the estimation due to the growing oscillation. This is why the effective range of the Wilson parameter is approximately $(0.8, 1.0)$. The estimation result are given in Fig 3.

We report the results of p_1 estimation by p_1^*, shown in Fig 4. We find that, in the 1-parameter ansatz, the value $r = 0.8$ produces the best estimation among the three typical values $r = 0.8, 0.9$ and 1.0. In the 2-parameter case, however, the ansatz $r = 0.8$ produces a somewhat unstable and oscillatory sequence. This may be a sign that the smaller r is not adequate for estimation using higher order derivatives.

Overall, we found that as r gets smaller, the region of continuum scaling observable in $\bar{\beta}_{n>}$ becomes wider, but $\bar{\beta}_{n>}$ and its derivatives begin to show oscillation at the slightly smaller value of $r = 1$. In contrast, when r is larger ($r > 1$), the effective region of $\bar{\beta}_{n>}$ gets narrower and the scaling behavior becomes vague. We found that $r \in (0.8, 1.0)$ provides a good estimation up to the 50th order. As in the cases frequently met with the Ising models, the estimation of the dynamical mass was superior to the estimation of the exponent p_1.

III. CONCLUDING REMARKS

We found that the cancellation of the linear divergence in $\bar{\beta}_{n>}$ remains effective under the δ expansion. As a consequence, the true logarithmic behavior of bare coupling was observed in $\bar{\beta}_{n>}$. We remark that the confirmation is explicit for the range of Wilson parameter $r \in (0.8, 1) = I$. It remains unclear whether other values of r are essentially useless even when the order is large enough. The present 50th order study tells us, however, that other values are not effective for practical use. In the range of I, the estimation of the dynamical mass m_D is carried out in the 1- and 2-parameter ansatze and all the sequences indicate the convergence to the exact value. It is interesting to note that, from the 35th to 36th and from the 43rd to 44th orders, rather big changes happen for $r = 0.8$ in 2-parameter ansatz.

It would be interesting to examine the estimation with the use of the exact value of p_i $(i = 1, 2)$. In this case, we utilized PMS in a looser variation of (30), $[1 + p_1^{-1}\frac{d}{d\log t}]\bar{\beta}^{(1)}_{n>} + \frac{1}{2\pi} \sim 0$ for the 1-parameter ansatz and $[1 + p_1^{-1}\frac{d}{d\log t}][1 + p_2^{-1}\frac{d}{d\log t}]\bar{\beta}^{(1)}_{n>} + \frac{1}{2\pi} \sim 0$ for the 2-parameter ansatz. The results for $r = 1$ are shown in Fig. 5, along with the results in the previous full PMS protocol. In the 1-parameter ansatz, the two sequences had almost the same accuracy (present protocol with $p_1 = 1$ fixed gave a slightly better result). In the

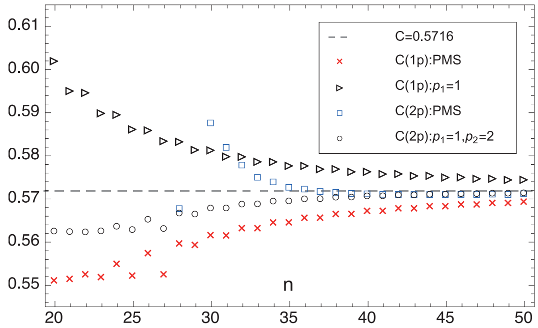

FIG. 5. Plots of estimation results for $r = 1$ in the 1-parameter ansatz with the input $p_1 = 1$ and 2-parameter ansatz with the inputs $p_1 = 1$ and $p_2 = 2$. For comparison, the results in 1- and 2-parameter ansatz in the previous section with the full PMS protocol are also plotted.

2-parameter ansatz, the result with the exact input $p_1 = 1$ and $p_2 = 2$ had better behavior to the orders of 20th or so. However, the two sequences tended to have similar behaviors at larger orders. From the various results so far obtained, the accuracy in the Gross-Neveu model with Wilson fermion is not as good as that in the Ising models. From numerical tests, this is roughly understood to stem from the behaviors of $\bar{\beta}^{(k)}_{n>}$ $(k = 1, 2, \cdots)$ in that the scaling behavior is not so clear to a few tens of orders. The reason behind this would be that non-oscillation of relevant functions needs r around the value $r \sim 1$ and in the region the lattice artifact remains effective.

[1] H. B. Nielsen and M. Ninomiya, Nucl. Phys. **185**, 20 (1981); Phys. Lett. **B105**, 219 (1981).
[2] K. G. Wilson, New Phenomena In Subnuclear Physics, ed. A. Zichichi, (Plenum Press, New York), Part A, 69 (1977).
[3] See for example, D. B. Kaplan, arXiv: 0912.2560 [hep-lat].
[4] H. Yamada, Phys. Rev. **D76**, 045007 (2007); Phys. Rev. **E90**, 032139 (2014) (arXiv:1407.2100 [hep-lat] (2014)).
[5] H. Hashiguchi, K. Hoshino and H. Yamada, Phys.Rev. **D77**, 085003 (2008).
[6] H. Yamada, J. Phys. **G36**, 025001 (2009).
[7] D. J. Gross and A. Neveu, Phys. Rev. D10, 3235 (1974).
[8] Our error in ref. [6] stemmed from a naive computational mistake. We also found that the constant C_2 appearing in eq. (62) has a typographical error and should be corrected to $C_2 = \int_{-\pi}^{\pi} \frac{d^2p}{(2\pi)^2} \left[\frac{r \sum_\mu (1-\cos p_\mu)}{(r \sum_\mu (1-\cos p_\mu))^2 + \sum_\mu \sin^2 p_\mu} \right]^2$. In fact, the constant C_2 in ref. [6] is nothing but c_2 in the present paper. All results in ref. [6] are, however, correct.
[9] P. M. Stevenson, Phys. Rev. **D23**, 2916 (1981).
[10] J-L. Kneur, A. Neveu and M. B. Pinto, Phys. Rev. A**69**, 053624 (2004).